Analysis and Experimental Of 3-Dimentional AOA with Directional Antenna on Narrowband MIMO Capacity

Charinsak Saetiaw[1], Saksit Summart[2], Chanchai Thongsopa[3]
[123](School of Telecommunication Engineering, Suranaree University of Technology, Thailand)

ABSTRACT: *Recently, many works have considered a physical properly of antenna in MIMO channel models, such as radiation pattern effective for MIMO system. However, effect of antenna for MIMO with different algorithms is required and also with different environments of signal behavior at each end of the link. Thus, a traditional antenna such as Omni-directional antenna generally is used to design MIMO systems. In this paper, we analyze the performance of directional antenna in different environment of signal spread for multiple-input-multiple-output (MIMO). We incorporate 3-dimensional (3D) of signal spread matching with directional antenna into a narrow-band MIMO channel model separately. This channel model allows us to investigate effect of distribution of signal coming to antenna combined with antenna radiation pattern to MIMO capacity in various propagation environments. We perform MIMO capacity simulations of a system with various antennas radiation pattern property. Uniform and peaky distribution models of angle of arrival (AOA) in azimuth and elevation planes are used in the simulations. We have shown that directional antennas reduce the narrow-band MIMO capacity when the AOA is uniformly distributed. If the AOA is peaky distributed, such as Laplacian distribution or Gaussian distribution, the narrow-band MIMO capacity is improved when the directional antennas with proper alignment to the mean AOA. However, radiation pattern will show some limitation of the antenna properties, such as gain and beam-width will affect to the capacity. This will trade off with limit an antenna for difference environment of propagation for MIMO by gain and beam-width. The proposed model is validated by narrow-band MIMO capacity measurements. Omni-directional monopole and Yagi-Uda with different gain and beam-width is used in the experiments. The experiments are performed in an anechoic chamber for reference and compared with indoor and outdoor scenario. The result verifies that the capacity with directional antenna is greater than isotropic capacity in proper scenarios.*

Keywords: *channel capacity, 3D-radiation pattern, multiple-input multiple-output (MIMO) system*

I. INTRODUCTION

It has been shown that systems with multiple antennas at both transmitter and receiver, called MIMO systems, linearly increase the capacity of a wireless link with the number of antennas [1]. The MIMO systems exploit the channel uncertainty to create multiple independent paths between the transmitter and receiver. The uncertainty of the channel is significantly influenced by fading phenomena of the wireless channel. Fading correlation is considered to be a major factor that reduces the MIMO capacity [2]. The MIMO capacity also depends On array element radiation patterns [3-6]. Unlike the fading Correlation, the radiation Patterns do not depend on a propagation environment.

Analysis performance of antenna design in a propagation channel for MIMO and antenna diversity systems has become many of publications. The resulting understanding has led to the practice of designing antenna arrays whose element radiation patterns are nearly orthogonal, as such a criterion leads to good performance in multi-antenna systems under specific assumptions such as the propagation environment. In practically, design of the antenna is likely to be used in different environments, such as indoor, outdoor, office and so on. The question is which type of antenna will improve in those environments. However, many works have recently reported best antenna characteristics for MIMO systems operating in a specific propagation environment [7], [8]. Furthermore, to compare antennas performance is not an easy task, since it is difficult to replicate the same channel conditions for different measurements. The solution for antenna properties must be optimal for the specific propagation channel that they considered. While these reported techniques are usually discovered, they need to consider the transmitted and received antenna characteristics together but the designs are interdependent.

This paper presents MIMO capacity results for directional antenna arrays in relevant environments using in- and outdoor environment and proposes a simplify model for analyze the antenna radiation characteristics based on stochastic characteristics of the propagation at receiver. We generalize the channel model so that it can take 3-dimension or 3D antenna property including antenna pattern effect on the system capacity into consideration.

There are two major contributions in this paper.

i) Investigate the effect of directional antenna with combined AOA distribution on the MIMO capacity in difference environment by simulations.

ii) Verify the simulation results by measurement in the real propagation scenarios compare with a result from simulations.

This paper is organized as follow. The next section, the proposed channel model of special correlation with directional antenna and propagation spread is discussed for multiple antenna systems. Simulations of the MIMO capacity in various propagation environments are presented in section three. Section four will report the results from our MIMO channel measurements and finally, the simulations comparing results will be reported.

II. ANALYSIS MIMO MODEL

2.1. Narrow-bands MIMO model

In this section, a brief review of "one-ring" channel model is given. Then, the proposed model of the MIMO system with the effect from pattern of directional antenna is discussed. The end of this section presents a technique for MIMO capacity calculation with effect of both antenna pattern property and a spread of AOAs.

Let $\mathbf{x}$ be a vector of the transmitted signals with n_T transmit antennas and $\mathbf{y}$ be a vector of the received signals with n_R receive antennas. Then the MIMO system model [1],[2],[9] is given by

$$\mathbf{y} = \mathbf{Hx} + \mathbf{n} \quad (1)$$

Where $\mathbf{n}$ is an $(n_R \text{x} 1)$ additive noise vector introduced at the receiver and $\mathbf{H}$ is an $(n_R \text{x}\, n_T)$ channel matrix.

The following assumptions are made in order to compute channel capacity for this model.

i) $\mathbf{H}$ Is a matrix of i.i.d. zero mean Gaussian random variables h_{ij} with variance σ_h^2.

ii) $\mathbf{n}$ is a vector of i.i.d. zero mean Gaussian random variables n_i with variance σ_n^2.

iii) The transmitter has knowledge of channel statistics and the receiver knows $\mathbf{H}$.

iv) The total transmit power P_{total} is allocated uniformly to each transmit antenna as $P = P_{total} / n_T$.

However, we consideration a model for a narrowband with a specify band of frequency spectrum. Let x and y be a transmitted and received signal respectively. The system model for a narrowband wireless system with single antenna at the both ends can be written as

$$y = hx + n \quad (2)$$

Where h and n are the channel impulse response and additive noise respectively.

However, to describe a channel in spherical coordinate that will be used for antenna radiation pattern or antenna gain and incident wave for either antenna will show in Fig. 1. An incoming signal will come over [0, 360] or [0, 2π] for azimuth plane (ϕ) and [0,180] or [0, π] for elevation plane (θ) respectively. We can be calculated antenna gain from the far-field radiation pattern in 3D using [10] we have,

$$G(\theta,\phi) = \frac{4\pi U(\theta,\phi)}{P} \quad (3)$$

Where $G(\theta,\phi)$ and P are antenna gain as a function of angle and total power respectively. $U(\theta,\phi)$ Is radiation intensity of antenna given by?

$$U(\theta,\phi) = \frac{1}{2\eta}\left[\left|E_\theta(\theta,\phi)\right|^2 + \left|E_\phi(\theta,\phi)\right|^2\right] \quad (4)$$

Where E_θ and E_ϕ is electric filed component of antenna. Substituting (4) into (3) gives

$$G(\theta,\phi) = k\left(\left|E_\theta(\theta,\phi)\right|^2 + \left|E_\phi(\theta,\phi)\right|^2\right) \quad (5)$$

Where $k = 4\pi / 2\eta P$.

The antenna radiation pattern is deterministic phenomena whereas the channel impulse responses are stochastic process. The incoming electromagnetic waves are stochastic process due to the randomness of the channel. Since the antenna is used for converting statistical electromagnetic waves to an electrical signal, the output electrical signal will be a stochastic process. However, the output stochastic process will not be the same with the input process because the antenna radiation pattern influences the input process as a transfer function. In other words, the randomness of the channel is altered by the antenna radiation pattern. The radiation pattern directly influences the capacity. In an ideal channel case, the antenna pattern is needed to be Omni-direction. However, in a certain propagation environment, the Omni-directional antenna may not be an optimal choice for maximizing the capacity.

A model for the channel including the effect of the radiation pattern is needed. We propose a MIMO channel model with antenna radiation pattern in 3-dimention. In this paper, the channel impulse responses, the angle of arrival and the antenna pattern can be modeled separately in the proposed model.

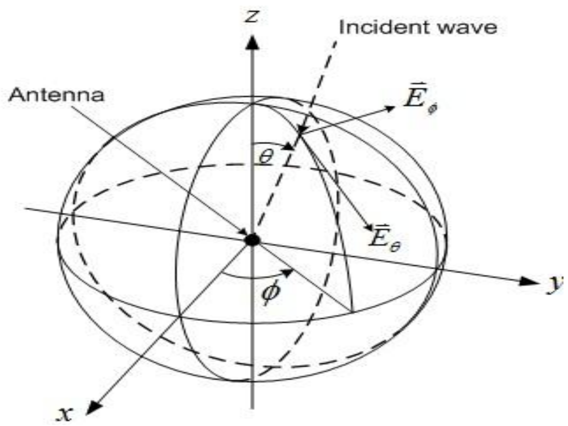

Fig.1 Spherical coordinate system.

For Omni-directional antenna, the direction of incoming signal derived as closed-form expressions. The distributions of AOA have a closed-form as a Uniform, Gaussian and Laplacian distribution have been introduced [11-13]. For these three distributions will using the AOA as indexing variables. So, the modified channel impulse response with the effect of the directional antenna and spread of AOA for a narrowband wireless system can be than written as

$$h_a = G(\theta,\phi)h \quad (6)$$

Where h is in frequency domain for narrowband system model.

The main advantage of the proposed model is that the channel impulse response and antenna pattern for different environments of AOA can be treated as one single function or separately depend on environment selected. The channel impulse response can be obtained from either a wireless channel measurement [7] or an analytic model [6],[14-16]. Whereas either a full wave electromagnetic simulation or antenna radiation pattern measurement can be used to obtain radiation or antenna gain pattern. By using (6) for the modified channel impulse responses with antenna pattern and a spread of AOA, each row of the channel matrix is given by

$$h_i^a = \left[G_i\,(\theta_1,\phi_1)h_{i1} \quad \ldots \quad G_i\,(\theta_{n_T},\phi_{n_T})h_{in_T}\right] \quad (7)$$

Where $G_i\,(\theta_i,\phi_i)$ is the radiation pattern of i-th receive antenna. Hence, the channel matrix with the effect of receive antenna radiation patterns and a spread of AOA can be written as

$$\mathbf{H}_a = \begin{bmatrix} h_1^a & h_2^a & \dots & h_{n_T}^a \end{bmatrix}^T \tag{8}$$

The MIMO system model in (1) with the effect received antenna radiation pattern and AOA can be written as

$$\mathbf{y} = \mathbf{H}_a \mathbf{x} + \mathbf{n} \tag{9}$$

The narrowband MIMO capacity is a function of the channel matrix will given by

$$C = \log \det\left(I_{n_T} + \frac{P}{\sigma_n^2} \mathbf{H}_a \mathbf{H}_a^T \right) \tag{10}$$

Where P the signal is power and σ_n^2 is the noise power. To calculate the capacity with effect of directional antenna and a spread of AOA, random matrices are generated by using (7) each realization of the channel matrix is obtained by using (9) and (10) where the AOA for each receive antenna is generated based on environments scenarios selected.

2.2. Distributions Function of AOA

For 3D Model, the propagation distribution for both azimuth and elevation planes are independent and identically distributed (i.i.d.) random variables. However, the distribution of the propagation directions are defined for azimuth and elevation plane. So, in literature measurement results suggest three candidates for AOA distribution in azimuth plane, Uniform, Gaussian and double exponential or Laplacian distributions [17]. The uniform distribution, which assumes that all the incoming waves are come from all direction in the azimuth plane, with an independent random phase for each azimuth direction with equal probability. The other distribution function can be written as follows.

1) Gaussian function:

$$\psi(x) = A_1 \exp\left[-\frac{(x-\mu)^2}{2b^2} \right] \tag{11}$$

2) Double exponential function:

$$\psi(x) = \begin{cases} A_2 \exp\left[-\dfrac{\mu - x}{b^-} \right], x < \mu \\ A_2 \exp\left[-\dfrac{x - \mu}{b^+} \right], x \geq \mu \end{cases} \tag{12}$$

If the spread parameters b^- and b^+ are equal, the double exponential function become Laplacian function as show in Fig. 2. Where coefficients $A_1 = 1/\sqrt{2\pi b^2}$ and $A_2 = 1/2b$.

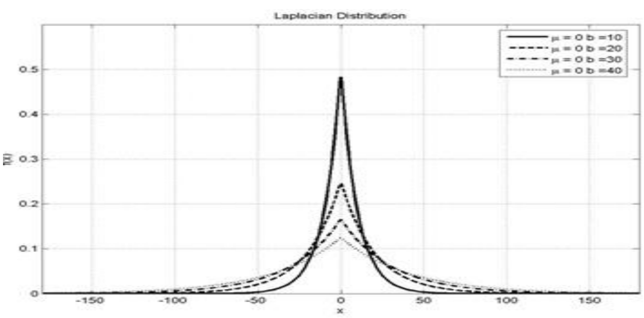

Fig. 2 Laplacian distribution.

III. SIMULATIONS

The MIMO capacity in (10) is evaluated using Monte Carlo simulations. Then, 10,000 instances of channel and collect the statistics of MIMO channel capacity were generated. In the simulations, 4 transmits and 4 receive antennas are used at the both ends. The signal to noise ratio (P/n) is calculated from a result of measurement that will discuss for detail later. The AOAs are generated using Uniform, Gaussian and Laplacian distribution in both azimuth and elevation plane depend on scenarios that will be describe as,

Scenario I – a measurement has been setting up in a laboratory room that has a desk and partition. The measurement space is 15.00m. x 7.00m. x 3.00m., as shown in Fig. 3. So, the distribution in azimuth plane is used and elevation will be uniformed on both planes.

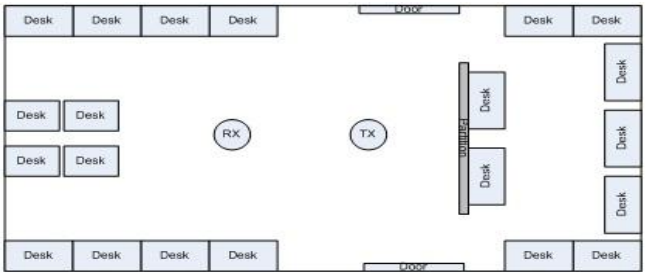

Fig. 3 Diagram of TX and RX location for indoor scenarios.

Scenario II – a measurement has setting up in a parking yard with a wide area opened. So, the distribution in azimuth plane using a peaky distribution with spread parameter is normal distribution. So, we will use both Gaussian and a double-sided exponential function with equal spread parameters or Laplacian on both planes in this scenario.

For AOA in 3D model, we will combine the AOA of the incoming multipath at the receiver both spherical angles θ and ϕ. The joint pdf $p(\theta,\phi)$ is written in terms of the conditional pdf of θ for a given ϕ; $p_\theta(\theta|\phi)$, and the marginal pdf $f_\phi(\phi)$ Thus,

$$p(\theta,\phi) = p_\phi(\phi) f_\theta(\theta|\phi) \tag{13}$$

So, the result of distribution of AOA in both azimuth and elevation plane can be written as,

1) Gaussian function:

$$\psi(\theta,\phi) = B_1 \exp\left[-\left(\frac{(\theta-\mu_\theta)^2}{2b_\theta^2} + \frac{(\phi-\mu_\phi)^2}{2b_\phi^2} \right) \right] \tag{14}$$

2) Double exponential function:

$$\psi(\theta,\phi) = \begin{cases} B_2 \exp\left[-\left(\dfrac{\mu_\theta - \theta}{b_\theta^-} + \dfrac{\mu_\phi - \phi}{b_\phi^-} \right) \right], \theta < \mu_\theta, \phi < \mu_\phi \\ B_2 \exp\left[-\left(\dfrac{\theta - \mu_\theta}{b_\theta^+} + \dfrac{\phi - \mu_\phi}{b_\phi^+} \right) \right], \theta \geq \mu_\theta, \phi \geq \mu_\phi \end{cases} \tag{15}$$

When coefficients $B_1 = A_1^2$ and $B_2 = A_2^2$. The center of distribution and direction of antenna must point into the direction of the main lobe of antenna. So, the distribution will shift an angle that the distribution mainly distributed that match to main lobe of an antenna we used. For simulation, a monopole antenna is used as a reference scenario and other three type of Yagi-Uda are used to investigate the effect of antenna radiation pattern with difference AOA distribution to the channel capacity.

The 3D radiation patterns of antennas are obtained from CST microwave studio 2009. The radiation pattern in the simulations, 5-element, 9-element, 13-element Yagi-Uda antennas are show in Fig. 4 and Fig. 5 for azimuth and elevation plane respectively.

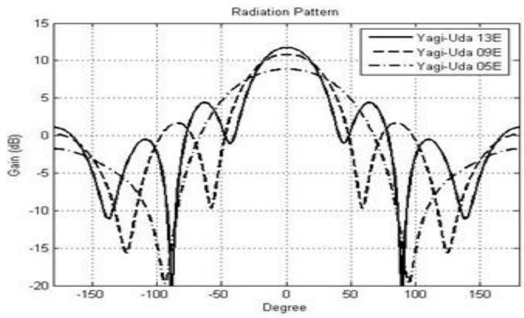

Fig. 4 The radiation pattern for Yagi-Uda on azimuth plane.

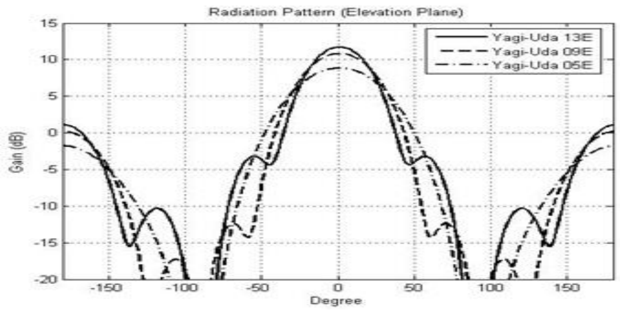

Fig. 5 The radiation pattern for Yagi-Uda on elevation plane.

The actual antenna pattern properties such as gain and HPBW from measurement compare to a result from CST is similarly on both azimuth and elevation planes as show in table 1 and table 2. Where the gains are with respect to Omni-directional antenna in dBi and HPBWs are in degrees. Antennas at receiver are equipped with uniform linear arrays (ULA) of the same type antennas. Furthermore, it is assumed that antenna spacing at both sides is the same at transmitter and receiver, each has four antennas.

The MIMO capacities were compared in terms of the Complementary Cumulative Distribution Functions (CCDF). The performance of each antenna type is varied by different scenarios referring to the different AOA distribution and the outage capacity observation. The channel capacity at a given outage probability q, denoted by C_q. The 10% outage channel capacities will be written as $C_{0.1}$.

Table 1. Antenna property from CST for simulation.

Antenna Type	Azimuth-HPBW (Degree)	Elevation-HPBW (Degree)	Gain (dBi)
Isotropic	-	-	1.00
Yagi-05E	86.4	59.0	8.84
Yagi-09E	58.8	48.0	10.83
Yagi-13E	44.9	40.0	11.70

Table 2. Actual antenna property used in measurement.

Antenna Type	Azimuth-HPBW (Degree)	Elevation-HPBW (Degree)	Gain (dBi)
Monopole	95.0	85.0	4.32
Yagi-05E	84.0	60.0	8.58
Yagi-09E	56.0	50.0	9.71
Yagi-13E	45.0	40.0	10.55

In order to access the capacity performance of directional antennas, the downlink of a point-to-point narrowband MIMO system is considered, operating at the frequency of 2.45 GHz. It is assumed the 3D scattering environment can be represented by a scenarios selected as describe before.

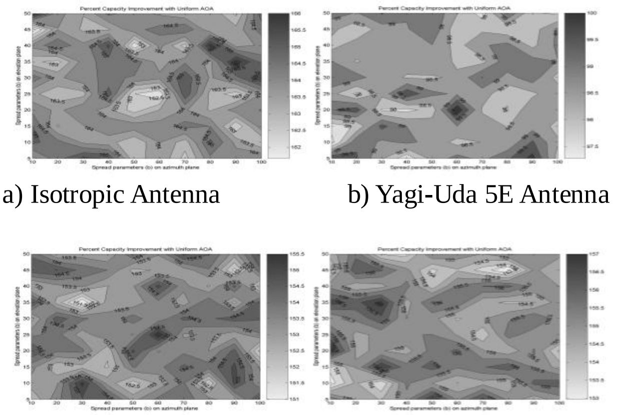

a) Isotropic Antenna b) Yagi-Uda 5E Antenna

c) Yagi-Uda 9E Antenna b) Yagi-Uda 13E Antenna

Fig. 6 Percent capacity outage with different spread parameter on 3D for scenarios I with Uniform AOA.

3.1 Scenario I

In this scenario, a distribution of AOA is uniformed on both planes. We generate channel with a distribution of AOA for 10000 instants. The AOAs are concentrated around the mean. The spread parameter is a parameter to control the randomness of the AOA. So, the result of the 10% outage channel capacities counted from CCDF will be compare to ideal case of isotropic antenna with different spread parameter of AOA distribution on azimuth and elevation plane will be investigated.

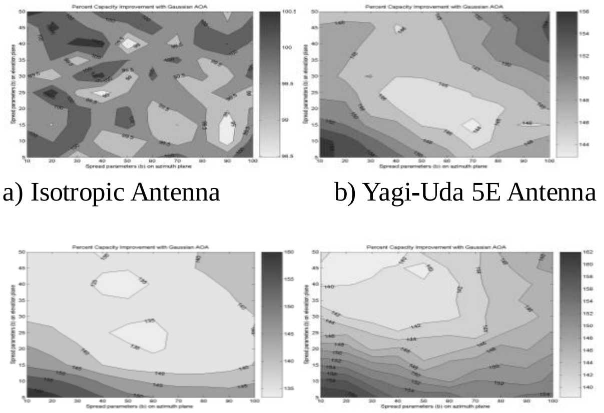

a) Isotropic Antenna b) Yagi-Uda 5E Antenna

c) Yagi-Uda 9E Antenna b) Yagi-Uda 13E Antenna

Fig. 7 Percent capacity outage with different spread parameter on 3D for scenarios II with Gaussian AOA.

The spread parameter between 10 to 100 degree on azimuth and 5 to 50 degree on elevation plane has been investigated. The 10% outage channel capacities for four types of antenna show in Fig. 6. The capacity is about 166%, 157% and 155% for 5E 9E and 13E Yagi-Uda antenna. All capacity is greater than the ideal case due to the gain of each antenna but not affect a spread of AOA changed.

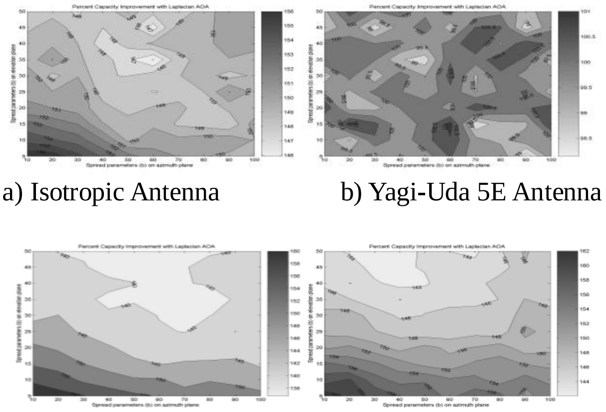

a) Isotropic Antenna b) Yagi-Uda 5E Antenna

c) Yagi-Uda 9E Antenna b) Yagi-Uda 13E Antenna

Fig. 8 Percent capacity outage with different spread parameter on 3D for scenarios II with Laplacian AOA.

3.2 Scenario II

In this scenario, the antenna is located so that the direction of maximum directivity is aligned with the mean of AOA of the Yagi-Uda antenna is used. The 10% outage channel capacities in (8) for all antenna types are shown in Fig. 7 and 8 for Gaussian and Laplacian AOA environment respectively.

It can be seen that the directional antennas maximize the system capacity show in Fig. 7 for Gaussian AOA. of the Yagi-Uda 5E , Yagi-Uda 9E and Yagi-Uda 13E is about 156%, 162% and 160% more than the ideal case. For Laplacian AOA in Fig.8, The result of Yagi-Uda 5E , Yagi-Uda 9E and Yagi-Uda 13E is about 156%, 162% and 160% more than the ideal case.

In this scenario, the capacity improvement is varied with a spread parameter in both planes. When the spread increases, it decreases the capacity on both ways.

IV. EXPERIMENTAL MEASUREMENTS

In this section, the capacity of a directional antenna, 5-elements 9-element and 13-elements Yagi-Uda, is measured. A Monopole antenna is used in the experiment for comparison with those three Yagi-Uda antennas. The 4-monopole array is used in the experiment as a transmit antenna. At the receiver, 4-Yagi-Uda array is used. The system is 4x4 MIMO.

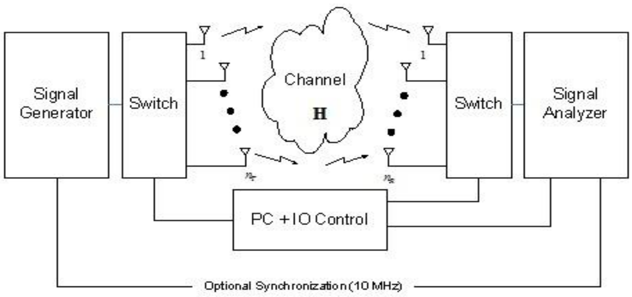

Fig. 9 Diagram of narrowband MIMO channel measurement system.

The block diagram of the capacity measurement system is shown in Fig. 9. The capacity measurements are performed by using the signal scheme in [18]. This signal is loaded into the E4433 signal generator. The received signals are store in the signal analyzer MXA9020A.

Table 3. Mutual Coupling level (S21).

Distance(Lambda)	Monopole	Yagi-05E	Yagi-09E	Yagi-13E
d=0.5	-34.73	-22.49	-23.27	-21.10
d=1.0	-36.41	-31.42	-30.91	-25.23
d=1.5	-46.20	-35.42	-34.05	-32.02
d=2.0	-43.49	-42.39	-41.52	-39.25
d=2.5	-50.21	-41.04	-41.86	-54.28
d=3.0	-44.42	-48.78	-52.52	-41.12
d=3.5	-52.33	-42.03	-67.43	-47.67
d=4.0	-53.16	-48.21	-62.91	-52.91

The antenna separations in the array are determined by mutual coupling measurements measuring in an anechoic chamber for monopole and all type of Yagi-Uda. The mutual coupling with various antenna separations is shown in table 3. Normally, the mutual coupling will effect to capacity when antenna space less than $\lambda/2$. So, the mutual coupling is less than -40 dB when the antenna separation is greater than 2λ. Finally, we choose the antenna separation of 2λ in the experiments to neglect the mutual coupling [19-20].

4.1 MIMO Capacity Calculation.

A comparison of the MIMO capacity achieved by each type of antenna array must be made using measurements from various scenarios. Directive antennas may increase SNR and also reduce the multipath signals that can be received by the antennas at the same time. To separate these two effects we firstly quantify whether there is a MIMO capacity reduction with directive antennas at constant SNR. To make a fair comparison shown in simulation, a monopole antenna closed to an isotropic antenna in all measurement scenarios is used to compare result with a simulation. Average channel capacity of monopole is measured as reference for normalized as follows.

A reference SNR measurement is made at each scenario using monopole ULAs with antenna spacing of 2λ. Mutual coupling is assumed to have negligible effect on receiver SNR for such large spacing. The reference measurement is made using the same grid positions and frequencies used for all site measurements. A reference noise variance is computed as before while the reference channel variance is computed as [21]

$$\sigma^2 = \frac{1}{n_T n_R}\sum_{i=1}^{n_T}\sum_{j=1}^{n_R}\left|h_{ij}\right|^2 \qquad (17)$$

The normalized ensemble average channel capacity is then computed as

$$\overline{C_N} = \frac{\overline{C_H}}{C(\sigma_{h,r}^2, \sigma_n^2)} \qquad (18)$$

Where $C(\sigma_{h,r}^2, \sigma_n^2)$ is the i.i.d. Gaussian channel capacity corresponding to the reference SNR measurement and computed by Monte Carlo simulation of the system defined in Section 3. The computed reference channel capacity is assumed to be able to achieve in the best case scenario of no mutual coupling and no channel correlation. This capacity normalization is a departure from the traditional method in which the measured channel matrices are normalized and SNR is scaled freely.

4.2 Field Measurement Procedure

Table 4. Measurement parameter for all scenarios

Parameter	Value
Transmitter antenna gain	4.32dB
Receiver antenna gain (Yagi-Uda 13E)	10.55dB
Receiver antenna gain (Yagi-Uda 09E)	9.71dB
Receiver antenna gain (Yagi-Uda 05E)	8.58dB
Receiver antenna gain (Monopole)	4.32dB
Distance from TX. ant. To RX. ant.	3.0 m.
Total transmission cable loss	-11.48dB

A measurement campaign is performed by using the QPSK signal generator that broadcasts a 50 MHz IF excitation signal at 2.45 GHz from each transmit antenna. The transmitted signal from each antenna is captured at each receive antenna by using a manual-switch. For far-field measurement, this transmitter and receiver will have 3 meter distance. A MXA9020A signal analyzer was used to measure a propagation gain that is used in this paper. A complete calibration of each radio's gain, phase noise and frequency offset was performed prior to field measurements.

It has been shown that the statistical property of AOA in outdoor propagation environment has peaky characteristic [22]. The measurement parameters are shown in table 4.

4.3 Measurement Results

This section presents the results from an indoor and outdoor measurement campaign using a measurement instrument test-set with the Yagi-Uda and monopole antennas. Measured channel capacity results from difference measurement scenarios are presented to show the effect of antenna radiation pattern and AOA distribution in environment. Before using the measurement result, it must normalize capacity as show in section 4.1. An average SNR at receive antenna from all measurement scenario as scenario I, scenario II and anechoic chamber are shown in table 5.

A reference SNR measure in chamber that will extremely have direct line of sight signal. That result show a difference scattering effect to SNR for both scenarios.

Table 5. Average receive power from measurements.

Antenna Type	Scenario I	Scenario II	Chamber
Monopole	-46.18	-46.33	-46.26
Yagi-05E	-43.56	-40.18	-39.49
Yagi-09E	-42.05	-38.87	-38.32
Yagi-13E	-40.76	-37.32	-37.20

Table 6. Improvement of 10% outage capacity from measurements.

Antenna Type	Scenario I	Scenarios II	Chamber
Monopole	100%	100%	100%
Yagi-05E	116%	143%	131%
Yagi-09E	134%	156%	141%
Yagi-13E	136%	164%	147%

However, a comprehensive set of results is presented for both scenarios. A fair comparison of MIMO performance is made between the Yagi-Uda and the reference monopole from simulation result as shown in table 6. A directional antenna in scenarios not be improved MIMO capacity but in scenarios II, directional antenna will improve MIMO capacity. Finally, directional antenna that has gain and direction match to AOA spread will improve MIMO capacity in condition as the direction of antenna is correctly.

V. CONCLUSIONS

This research proposes proposed the channel model for MIMO capacity calculation. The proposed model can be used to calculate the MIMO capacity with the presence of 3D antenna radiation pattern.

The proposed model allows us to model the 3D antenna pattern. The elements spacing are 2λ for decrease effect of mutual coupling. However, not only radiation pattern of the element influences the narrowband MIMO capacity but also the statistical property of AOA. We have shown that directional antennas are not attractive for MIMO systems in a scenario where the randomness of AOA is high. In a scenario with AOA concentrating on a single value, the antenna position is crucial to the capacity. If the antenna is point into the mean AOA, then the capacity is increased. The results from measurement show that the AOA and antenna radiation pattern influence narrowband MIMO capacity from simulation be confirmed.

On the other hand, in rich scattering environments, the power gain of directional antennas is no more helpful, since the signal power is dispersed over a large extent of directions. The limited beam-width of directional antennas will decrease in the effective angular spread which severely increases the correlation. Therefore Omni-directional antennas outperform in these situations. These results suggest the following general guidelines for selection of antenna type. Our results show that choosing the suitable antenna, operating SNR and antenna spacing are other factors that should also be considered together with the spread of AOA.

VI. ACKNOWLEDGEMENTS

This work was supported by Suranaree University of Technology (SUT) and advised by Ms. Natthanan Summat on the paper report writing.

REFERENCES

[1] G.J. Foschini and M.J. Gan, On limits of wireless communications in fading environment when using multiple antennas, Wireless Personal Communications, 6(3), 1998, 311-335.
[2] D.S. Shiu, G.J. Foschini, M.J. Gans and J.M. Kahn, Fading correlation and its effect on the capacity of multi-element antenna systems, Proc. IEEE 1998 International Conference on Universal Personal Communications, 1998, 429-433.
[3] K. Yu and B. Ottersten, Models for MIMO propagation channels: A review, Wirel. Commun. Mob. Comput., 2(7), 2002, 653–666.
[4] B. Wang, and A.G. Burr, Effect of element radiation patterns on the capacity of MIMO system, Proc. IEEE Int. Symp. on Microwave, Antenna, Propagation and EMC Tech. for Wireless Comms, 2005, 1448 – 1451.
[5] C. Saetiaw, A. Intrapanich, C. Thongsopa, Effect of Spatial Correlation with Directional Antenna on MIMO Capacity, Proc. of ISAP2007, 2007, 1334-1338.
[6] H.S. Rad and S. Gazor, The impact of non-isotropic scattering and directional antennas on MIMO multicarrier mobile communication channels, IEEE Transactions on Communications, 56(4), 2008, 642–652.
[7] D. Chizhik, J. Ling, P.W. Wolniansky, R.A. Valenzuela, N. Costa, and K. Huber, Multiple-input-multiple-output measurements and modeling in Manhattan, IEEE J. Sel. Areas Commun., 21, 2003, 321–331.
[8] K.I. Pedersen, P.E. Mogensen, and B.H. Fleury, Power azimuth spectrum in outdoor environments, Electron. Lett., 33(18), 1997, 1583–1584.
[9] I.E. Telatar, Capacity of multi-antenna Gaussian channels AT&T Bell Labs, Tech. Rep., 1995.
[10] C.A. Balanis, Antenna Theory: Analysis and Design, 3rd Edition, John Wiley & Sons Inc, 2005.
[11] K.I. Pedersen, P.E. Mogensen, and B.H. Fleury, A stochastic model of the temporal and azimuthally dispersion seen at the base station in outdoor propagation environments, IEEE Trans. Veh. Technol., 49(2), 2000, 437–447.
[12] Q.H. Spencer, B.D. Jeffs, M.A. Jensen, and A.L. Swindelhurst, Modeling the Statistical Time and Angle of Arrival Characteristics of an Indoor Multipath Channel, IEEE Journal on Selected Areas in Communications, 18, 2000, 347-3602000.
[13] F. Adachi, M. Feeny, A. Williamson, and J. Parsons, Cross-Correlation between the Envelopes of 900 MHz Signals Received at a Mobile Radio Base Station Site, IEE Proceedings Pt. F, 133, 1986, 506-512.
[14] W.C.Y. Lee, Effects on correlation between two mobile radio base-station antennas, IEEE Trans. Commun., 21, 1973, 1214–1224.
[15] J. Salz and J. Winters, Effect of Fading Correlation on Adaptive Arrays in Digital Mobile Radio, IEEE Transactions on Vehicular Technology, 43, 1994, 1049-1057.
[16] C. Saetiaw, A. Intarapanich, C. Thongsopa, Relations Between 3-Dimensions Antenna Pattern and Narrowband MIMO Capacity, Proc. Microwave Conference, APMC2007, 2007, 1 – 4.
[17] K. Kalliola, K. Sulonen, H. Laitinen, O. Kivek¨as, J. Krogerus, and P. Vainikainen, Angular power distribution and mean effective gain of mobile antenna in different propagation environments, IEEE Transactions on Vehicular Technology, 51(5), 2002, 823–838.
[18] D.W. Browne, W. Zhu, and M.P. Fitz, A signaling scheme and estimation algorithm for characterizing frequency selective MIMO channels, Proc. IEEE Veh. Technol. Conf., 2005.
[19] T. Svantesson and A. Ranheim, Mutual coupling effects on the capacity of multielement antenna systems, Proc. IEEE ICASSP, 2001, 2485–2488.
[20] I. Gupta and A. Ksienski, Effect of mutual coupling on the performance of adaptive arrays, IEEE Trans. Antennas Propag., 31, 1983, 785–791.
[21] D.W. Browne, M. Manteghi, M.P. Fitz, Y. Rahmat-Samii, Experiments With Compact Antenna Arrays for MIMO Radio Communications, Antennas and Propagation, IEEE Transactions on , 54(11), 2006, 3239-3250.
[22] M. Alsehaili, S. Noghanian, D.A Buchanan and A.R. Sebak, Angle-of-Arrival Statistics of a Three-Dimensional Geometrical Scattering Channel Model for Indoor and Outdoor Propagation Environments, IEEE Antennas and Wireless Propagation Letters, 9, 2010, 946-949.